International Research Journal of Biological Sciences ISSN 2278-3202
Vol. **15(3),** 15-27, August **(2026)** *Int. Res. J. Biological Sci.*

Exploring Antiviral Chemical Space for the Discovery of Novel RNA-Dependent RNA Polymerase inhibitors against Japanese Encephalitis Virus

Akshay Kumar Shukla[1], Mohd Saeed[2], Vivek Dhar Dwivedi[3] and Ramesh Chandra Tripathi[1*]
[1]Department of Biological Sciences, Faculty of Science and Environment, Mahatma Gandhi Chitrakoot Gramodaya Vishwavidyalaya, Chitrakoot, Satna, India
[2]Department of Biology, College of Science, University of Hail, Hail, Saudi Arabia
[3]Bioinformatics Research Division, Quanta Calculus, Greater Noida, UP, India
rctbsmgcgv2@gmail.com

Available online at: www.isca.in, www.isca.me
Received 20th June 2026, revised 15th July 2026, accepted 7th August 2026

Abstract

This research focuses on Japanese encephalitis virus (JEV), one of the most serious mosquito-borne flaviviruses that cause neuroinvasive disease in humans. Despite the wide use of vaccines, there is still a high burden of JEV infections for which there are no good therapies. One of the main enzymes responsible for viral replication is the RNA-dependent RNA polymerase (RdRp), and it could be a good drug target. Thus, in the current research, we employed a structure-based virtual screening strategy to predict inhibitors of the JEV RdRp enzyme using the enzyme's crystal structure and Life Chemicals' antiviral library. Fifteen candidates were identified during the screening process and then re-scored using MM/GBSA calculations. After scoring using MM/GBSA values, the three top-ranking molecules (F3217-0045, F1951-0385, and F1951-0396), together with the reference inhibitor Galidesivir, underwent detailed analysis via molecular dynamics simulations. All three selected molecules interacted stably with the catalytically active sites in the ATP-binding pocket and exhibited higher binding affinity than the reference inhibitor. The trajectory analysis and trajectory-based MM/GBSA calculations indicated that all three selected compounds formed stable protein-ligand complexes over 100 ns of MD. Particularly, F3217-0045 had the best binding free energy (-84.95 ± 5.71 kcal/mol) among the three molecules, and F1951-0396 had the highest stability during the molecular dynamics simulation. Overall, the results presented constitute the discovery of promising lead molecules that inhibit JEV-RdRp and provide a basis for further experimental studies.

Keywords: Japanese encephalitis virus, RNA-dependent RNA polymerase, Virtual screening, Molecular dynamics simulation, Binding free energy.

Introduction

Despite the presence of potent vaccines against JEV, it continues to be one of the most common causes of viral encephalitis in Asia and the Western Pacific region[1–3]. JEV is an enveloped RNA virus that belongs to the genus Flavivirus, which is predominantly transmitted to humans by Culex mosquitoes, with pigs serving as amplifying hosts and ardeid birds as major reservoirs. Humans act as incidental dead-end hosts for JEV due to low viremia. Although almost 99% of infections are asymptomatic, symptomatic disease can progress to acute encephalitis with high fever, seizures, altered mental status, paralysis, and coma. Case fatality is 20-30% and about half of survivors have permanent neurological or psychiatric sequelae, emphasizing the urgent need for effective antiviral interventions[4]. JEV has a positive-sense single-stranded RNA genome of about 11 kilobases. The genomic RNA of the virus is translated to form a single polyprotein, which is cleaved to form three structural proteins (capsid, premembrane, and envelope) and seven non-structural proteins (NS1-NS5), which are essential for viral replication and disease causation[5,6]. The envelope glycoprotein among these proteins mediates host-cell attachment and membrane fusion, NS2B–NS3 is a serine protease and helicase essential for polyprotein processing, and NS1, NS4A, and NS4B are involved in replication complex formation and immune evasion[7]. These viral proteins have thus attracted considerable attention as therapeutic targets for the development of antiviral agents.

NS5 is the biggest and the most conserved protein among all other proteins encoded by the JEV genome. It consists of two domains: the N-terminal domain is the methyltransferase, which is engaged in RNA cap formation, and the C-terminal RNA-dependent RNA polymerase (RdRp) domain, which is responsible for RNA synthesis[8]. The RdRp possesses the standard right-handed structure, including the fingers, palm, and thumb domains, with typical flavivirus catalytic motifs. Mammalian cells lack RNA-dependent RNA polymerases; therefore, the enzyme represents an attractive antiviral target with good selectivity and low potential for host toxicity. Furthermore, high-resolution crystal structures of JEV RdRp have allowed structure-guided drug discovery and identification of small molecules targeting the catalytic pocket or neighboring allosteric sites[8,9].

Significant efforts have been made to find inhibitors of JEV RdRp. Nucleoside analogues such as favipiravir and related ribonucleoside derivatives act as alternative substrates for the polymerase and inhibit viral RNA synthesis, while a range of non-nucleoside inhibitors, identified by virtual screening and structure-based drug discovery, are thought to interfere with nucleotide binding or polymerase conformational dynamics[10–12]. Moreover, computational studies have revealed several chemical scaffolds, natural products, and repurposed antiviral molecules with promising binding affinity towards JEV RdRp catalytic domain. However, only a few of these candidates have been fully biologically validated and no RdRp-targeting antiviral has been approved for the treatment of Japanese encephalitis, which emphasizes the persistent need for novel lead molecules with improved efficacy and drug-like properties. Due to the essential role of RdRp in viral genome replication and its extraordinary structural conservation among flaviviruses, the enzyme serves as an attractive target for antiviral discovery. Hence, the present study was initiated to discover novel small-molecule inhibitors of the JEV RdRp from an antiviral-oriented chemical space enriched with compounds with documented antiviral properties. This work strives to identify promising lead candidates by prioritizing compounds with favorable predicted binding characteristics and interaction stability that may facilitate the future development of therapeutics against JEV.

Materials and Methods

Retrieval and Preparation of the Target Protein: The three-dimensional crystalline configuration of RNA-dependent RNA polymerase (RdRp) from the Japanese encephalitis virus (JEV), associated with adenosine triphosphate (ATP), was obtained from the Protein Data Bank (PDB ID = 4HDH)[8,13]. Protein preparation was done using the Protein Preparation Wizard tool in Schrödinger Maestro[14]. Water molecules that are exposed outside the ligand-binding site were stripped out; hydrogen atoms were added where they are missing; bond orders were specified; and the ionization state of the amino acids was optimized for physiological pH conditions. Missing side chains and loops were refined and then subjected to restrained energy minimization in the OPLS3e force field until the heavy atom root-mean-square deviation (RMSD) became 0.30 Å[15].

Antiviral Compound Library: For this study, we used the Life Chemicals Antiviral Screening Compound Library, which contains more than 15,400 small molecules that are structurally diverse. The library was constructed using a 2D fingerprint similarity approach against a reference set of 46,518 biologically active compounds (IC_{50}, K_i, or related activity values <10μM, or inhibition >25%) from therapeutically relevant antiviral assays. The reference compounds were obtained from the Binding DB, ChEBI, PubChem and ChEMBL databases and correspond to different viral species and their protein targets. Then, the Life Chemicals HTS Compound Collection was screened for analogs of these known antiviral molecules with a threshold of 80%. Tanimoto similarity based on MDL public key fingerprints, generating a focused antiviral screening library of over 15,400 unique compounds. The chemical structures of all compounds were put through LigPrep (Schrödinger LLC) to optimize geometry, generate proper ionization states at physiological pH, generate stereoisomers as needed, and minimize energy with the OPLS3e force field[16].

Receptor Grid Generation: The receptor grid was generated with the Glide Receptor Grid Generation module in Schrödinger Maestro[17]. The docking site was chosen to be the ATP-binding pocket as seen in the crystal structure. The grid center was defined as the centroid of the co-crystallized ATP molecule and the size of the enclosing and inner boxes were optimized to fully cover the ligand binding cavity and to allow flexible ligand placement during docking calculations.

Structure-Based Virtual Screening: The traditional hierarchical docking protocol was adopted for virtual screening utilizing the Glide component of the Schrödinger suite. Firstly, High Throughput Virtual Screening (HTVS) was performed on all compounds to filter out weak binders. The best 10% of compounds as per Glide Score were further used for SP docking. In the next step, the best 10% of SP docking were further used for Extra Precision (XP) docking in order to achieve highly reliable docking poses and docking scores. Compounds were sorted using their Glide XP scores, and the best compounds were chosen for further analysis in terms of binding free energies[18–20].

Binding Free Energy Estimation: The binding affinity of docked protein-ligand complexes was analyzed with the help of Prime MM-GBSA protocol from Schrödinger Suite[21]. The binding free energy (ΔGbind) was calculated using the VSGB implicit solvent model combined with the OPL3e force field. It is given as ΔG bind = Gcomplex - (Gprotein + Gligand), where Gcomplex is the free energy of the protein-ligand complex, Gprotein is the free energy of the isolated receptor, and Gligand is the free energy of the isolated ligand. The compounds were ranked based on the MM-GBSA binding free energy values and the top three compounds were chosen for further analysis through MD simulations.

Molecular Dynamics Simulation: The dynamic properties and conformational stability of selected protein-ligand complexes were studied by means of all-atom MD simulations with the use of the Desmond package from the Schrödinger software suite[22]. Before running the simulation, each docked complex was prepared using the default system builder to generate solvated models for long-timescale analyses. An explicit solvent model was created by putting each complex into an orthorhombic simulation box filled with TIP3P water molecules. To avoid artifacts arising from the periodic boundary condition, the distance between the exterior of the protein and the boundary planes of the box was kept at 10Å in each direction. The systems were neutralized with the required number of Na^+ or Cl^- ions, depending on the complex's charge. Moreover, a physiological ionic strength of 0.15M NaCl was added to mimic cellular conditions.

Prior to running the production simulations, each solvated system was subjected to energy minimization to eliminate unfavorable atomic clashes and steric strain arising from the preparation process. After energy minimization, the systems were gradually equilibrated using Desmond's multistep relaxation protocol. Such an approach allows the attainment of a stable thermodynamic state of the solvent, ions, and protein while minimizing structural deformations in the systems.

Production MD simulations were run using the isothermal-isobaric (NPT) ensemble to keep the pressure and temperature constant. Temperature was kept at 300K by the Nosé-Hoover chain thermostat, and pressure was maintained at 1.01325 bar by the Martyna-Tobias-Klein barostat[23,24]. These algorithms enable proper maintenance of thermodynamic parameters and realistic sampling of motions.

Electrostatic long-range interactions were calculated using the Particle Mesh Ewald (PME) method in order to take into account Coulombic forces accurately under the periodic boundary condition. Hydrogen bonds were restrained with the SHAKE algorithm, allowing for a stable integration time step[25]. Each system was simulated for 100 ns, with a 100 ps interval between coordinate saves, to further analyze the trajectory and study conformational stability, residue flexibility, intermolecular interactions, and other dynamic parameters.

Trajectory Analysis: The trajectories were analyzed using the Simulation Interaction Diagram (SID) tool of the Desmond software suite[22]. The structure stability was determined using the root mean square deviation (RMSD) of the protein backbone atoms and the ligand heavy atoms over the course of the simulations. The flexibility was estimated at residue level through the root mean square fluctuation (RMSF). Other descriptors such as the radius of gyration (Rg), solvent accessible surface area (SASA), and the number of intramolecular hydrogen bonds were recorded to assess the compactness and stability of the protein. The protein-ligand interaction patterns, consisting of hydrogen bonding, hydrophobic interactions, ionic interactions, π-π stacking, and water bridges, were determined along the trajectory to establish stable interactions that stabilized the ligand in the active site.

Trajectory-Based MM-GBSA Analysis: Trajectory based MM-GBSA calculations were performed using thermal_ mmgbsa.py script provided in Schrödinger package to estimate the dynamic binding affinity of the selected ligands[21]. The average binding free energy over the simulation was calculated from representative snapshots taken at regular time intervals from the MD trajectories. The obtained ΔG_bind values gave a quantitative measure of the stability of ligand binding considering receptor flexibility and solvent effects, therefore complementing the docking results and helping to identify the most promising lead compounds against JEV RdRp.

Results and Discussion

Virtual Screening and MM-GBSA-Based Selection of Lead Compounds: We used a hierarchical structure-based virtual screening workflow to screen the Life Chemicals Antiviral Screening Library for potential inhibitors of JEV-RdRp. Sequential filtering during the virtual screening process was effective in reducing the number of candidate molecules, resulting in a final set of 15 compounds with good docking characteristics. The shortlisted compounds were re-evaluated using MM-GBSA binding free energy calculations for a more reliable estimation of their binding affinity towards the catalytic domain of JEV RdRp (Table-1).

The compounds F3217-0045, F1951-0385 and F1951-0396 showed the best MM-GBSA binding free energies and were considered as the lead candidates for further analyses. Galidesivir, a broad-spectrum antiviral drug, was chosen as the reference inhibitor for comparison[26].

Molecular Interaction Analysis: Detailed analysis of the docked binding poses showed that all three lead compounds were well fitted in the ATP-binding cavity of the polymerase and formed multiple stabilizing interactions with the residues lining the catalytic pocket.

Among the selected molecules, F3217-0045 formed hydrogen bonds with Arg460 and Arg734, and additional electrostatic interactions involving Arg474, Lys463, Arg460 and Arg742 further stabilized the ligand in the binding site. The complex was also stabilized by hydrophobic interactions with Trp477, Ile476, Ala475, Val414 and Trp800, suggesting a high degree of nucleotide-binding pocket occupancy.

The second lead compound F1951-0385 showed a large interaction network with hydrogen bonding to Trp800, Arg460 and Arg742. Salt bridge interactions with Arg742, Lys463, Arg 460 and Arg474 offered further electrostatic stabilization, while hydrophobic interactions with Met345, Phe478, Ile476, Val414 and Trp800 enhanced ligand accommodation at the active site cavity. This compound was able to interact simultaneously with several positive charged residues, pointing to a very stable binding mode.

F1951-0396 showed the broadest interaction profile among the three lead candidates. The ligand formed hydrogen bonds with Arg474, Arg742, Arg460, Trp800 and Ser801 as well as several salt bridges with Arg460, Arg742 and Arg474. Hydrophobic interactions with Trp477, Ile476, Ala475, Val414, Trp800, and Ile802 provided additional stabilization of ligand binding. The presence of multiple persistent hydrogen bonds coupled with complementary electrostatic and hydrophobic interactions suggests that this compound adopted a very favorable binding orientation in the RdRp active site.

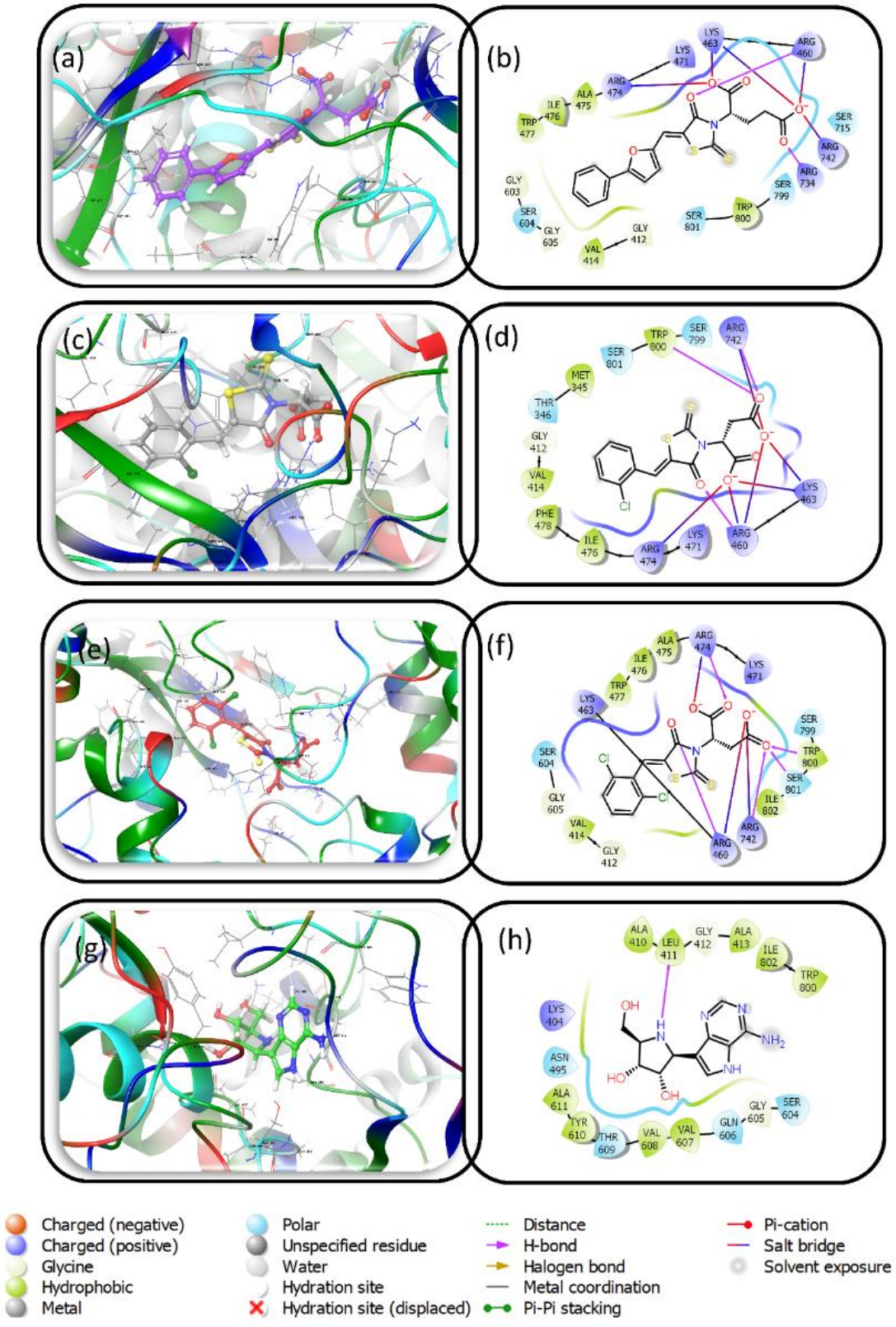

Figure-1: Binding modes of the selected lead compounds and the reference inhibitor in the active site of JEV RdRp. (a-b) F3217-0045 (c-d), F1951-0385 (e-f), F1951-0396 and (g-h) Galidesivir (reference) showing interactions with key catalytic residues.

Table-1: Virtual screening results for the top-ranked compounds identified against JEV RdRp following hierarchical molecular docking and MM/GBSA binding free-energy analysis.

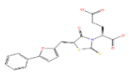	F3217-0045	-12.227	-65.70
	F1951-0385	-12.201	-59.39
	F1951-0396	-12.175	-58.48
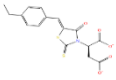	F1951-0043	-12.753	-58.43
	F0207-0620	-13.373	-58.17
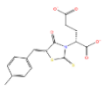	F0393-0638	-14.080	-58.03
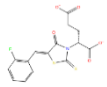	F1951-0361	-12.003	-57.89
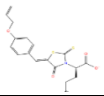	F1951-0246	-12.533	-57.78
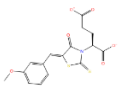	F1951-0063	-12.806	-57.50
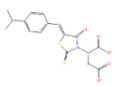	F1951-0423	-13.359	-56.85
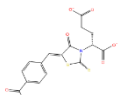	F1951-0346	-12.310	-54.39
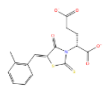	F1951-0012	-12.185	-52.48
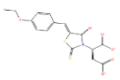	F1951-0077	-12.340	-50.55
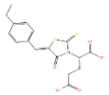	F1951-0044	-12.048	-48.90
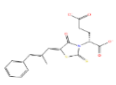	F1951-0442	-12.519	-48.06

In contrast, the reference inhibitor Galidesivir displayed a comparatively less complex interaction pattern. The reference compound formed one hydrogen bond with Leu411 and was mainly stabilized by hydrophobic interactions with Ala410, Leu411, Ala413, Tyr610, Val607, Val608, Ala611, Trp800 and Ile802. The reference complex showed no salt bridge interactions. The interaction profiles of the selected lead compounds were characterized by more hydrogen bonds and electrostatic interactions even though Galidesivir occupied the catalytic cavity of JEV RdRp, indicating the stronger molecular recognition in the ATP-binding pocket.

F3217-0045, F1951-0385 and F1951-0396 were selected for molecular dynamics simulations considering their good MM-GBSA ranking as well as their extensive interaction networks with catalytically important residues of JEV RdRp. These analyses were performed to evaluate the structural stability of the protein-ligand complexes and to investigate the persistence of the observed interactions under dynamic simulation conditions.

Molecular Dynamics Simulation

The structural stability of the three selected lead compounds (F3217-0045, F1951-0385 and F1951-0396) and the reference inhibitor (Galidesivir) in complex with JEV RdRp was studied by 100 ns molecular dynamics (MD) simulations.

RMSD Analysis: The overall conformational stability of the complexes was checked through monitoring the protein backbone and ligand RMSD during the simulation time Figure-2.

The F3217-0045–RdRp complex showed rapid equilibration in the initial phase of simulation with the protein backbone RMSD fluctuating in the range of 1.8–2.7Å in the 100 ns trajectory (Figure-2a). Between 50 and 70 ns, minor conformational fluctuations were observed, and then the protein stabilized without any significant structural drift. The RMSD of the ligand was within the range of about 1.2Å to 3.8Å, with temporary jumps between 25 and 45 ns, then followed by a slow decline and was stabilized at near 2.0 Å in the last phase of the simulation. The relatively low ligand RMSD after equilibration indicates that F3217-0045 maintained a stable binding pose within the catalytic pocket despite local conformational rearrangements.

The F1951-0385–RdRp complex showed the stable protein behavior as well, and the backbone RMSD values were mostly in the range of 1.2–2.6Å during the simulation period (Figure-2b). Within the first 10 ns the protein equilibrated and remained structurally intact thereafter. However, the ligand showed relatively larger fluctuations than the other screened compounds with RMSD values ranging from about 4.3 to 6.8 Å. A large increase in the ligand RMSD was observed between 45 and 65 ns, indicating the binding pocket went through a conformational rearrangement before stabilizing for the last part of the

simulation. The ligands do exhibit some movement, but this does not result in a corresponding increase in the protein RMSD, suggesting that the observed fluctuations are more likely a consequence of ligand reorientation rather than dissociation from the active site.

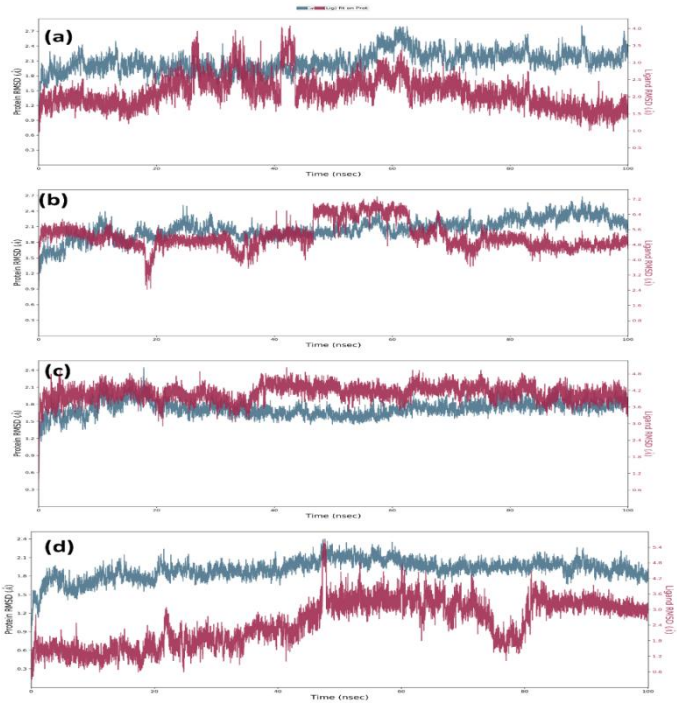

Figure-2: Protein backbone and ligand RMSD profiles of JEV RdRp complexes during 100 ns molecular dynamics simulation. (a) F3217-0045, (b) F1951-0385, (c) F1951-0396, and (d) Galidesivir.

Among the compounds studied, the F1951-0396–RdRp complex showed the highest structural stability (Figure 2c). The protein backbone RMSD converged fast in the first few ns and stayed stable between 1.5 and 2.1 Å for the entire simulation with only small fluctuations. Similarly, the ligand RMSD was very stable in the range of 3.6–4.5 Å without any sharp deviations. After a small conformational adjustment around 35-40 ns, both the protein and the ligand exhibited almost constant RMSD values throughout the simulation, indicating a well-equilibrated and highly stable protein-ligand complex.

The reference complex Galidesivir-RdRp showed similar stable protein backbone dynamics as seen in the screened compounds with RMSD values in the range of 1.6–2.2Å after initial equilibration (Figure-2d). The ligand RMSD was relatively low at the beginning of the simulation until 40 ns and then gradually increased between 45 to 60 ns suggesting a conformational rearrangement in the binding cavity. At ~75 ns there was a transient decrease in ligand RMSD and then the ligand assumed another stable conformation till the end of the simulation. Galidesivir remained bound to the active site throughout the trajectory, but its ligand RMSD profile suggested more positional flexibility than was observed for F3217-0045 and F1951-0396.

Residue Flexibility Analysis (RMSF): The residue-wise flexibility of the JEV-RdRp in complex with the three selected lead compounds and the reference inhibitor was evaluated by calculating the root mean square fluctuation (RMSF) of the Cα atoms over the 100 ns molecular dynamics simulation (Figure 3). The RMSF analysis provides a view of the local mobility of the amino acid residues, and helps to identify the flexible regions that may affect the protein stability and ligand binding.

The F3217-0045–RdRp complex displayed an overall low fluctuation profile with most of the residues having RMSF values less than 1.5 Å (Figure-3a). The pronounced fluctuations were predominantly located in the N-terminal region, where residues around 45–70 showed the highest mobility, reaching approximately 4.0Å. Additional localized fluctuations were observed around residues 190, 320, 470 and in the C-terminal segment (560–610). However, despite these flexible loop regions, the catalytic core of the polymerase was relatively rigid throughout the simulation, suggesting that binding of F3217-0045 did not induce significant structural perturbations.

Table-2: Protein–ligand interaction profiles of the selected lead compounds and the reference inhibitor within the ATP-binding pocket of JEV RdRp, showing hydrogen bonds, salt bridges, and hydrophobic interactions.

Complex	Hydrogen bond	Salt bridge	Hydrophobic residues
F3217-0045	ARG460, RG734	ARG474, LYS463, ARG460, RG742	TRP477, ILE476, ALA475, VAL414, TRP800
F1951-0385	TRP800, RG460, ARG742	ARG742, YS463, ARG460, RG474,	MET345, PHE478, ILE476, VAL414, TRP800
F1951-0396	ARG474, RG742, ARG460, TRP800, SER801	ARG460, RG742, ARG474	TRP477, ILE476, ALA475, VAL414, TRP800, ILE802
Reference_10445549	LEU411	–	ALA410, LEU411, ALA413, ILE802, TRP800, ALA611, TYR610, VAL608, VAL607

The bound complex of F1951-0385 also exhibited a stable fluctuation profile with most of the residues having the RMSF values in the range of 0.5 to 1.5Å (Figure-3b). The increased flexibility was observed in the regions of residues 40-60 and 140-160 with RMSF values close to 3.0Å. We also observed moderate fluctuations around residues 200, 320 and 470, while the C-terminal residues showed only a slow increase in mobility. Overall, the fluctuation pattern indicates that the structural integrity of the polymerase was preserved by the ligand binding, and the flexibility was limited mostly to the exposed loop regions. The F1951-0396–RdRp complex exhibited the most uniform RMSF profile of the systems studied (Figure-3c). The majority of residues stayed below 1.2Å, showing a good structural rigidity during the simulation. Although transient peaks were observed in the vicinity of residues 50–70, 140–160, 200, 320, 480 and 560, their amplitudes were relatively lower than those observed in the other complexes. Importantly, the residues forming the catalytic domain exhibited small fluctuations, implying F1951-0396 stabilized the polymerase during the simulation. This relatively homogeneous fluctuation profile is in agreement with the stable RMSD behavior observed for this complex.

The RMSF pattern of the Galidesivir–RdRp complex was similar to the screened compounds (Figure-3d). The peak fluctuations were observed to approach 3.5Å with an increased flexibility around residues 40-50 and 130-150. Moderate additional peaks were seen near residues 270, 320, 470 and 560, with a significant increase in fluctuation at the extreme C-terminal residues. The central catalytic region, however, was relatively low in mobility, suggesting that Galidesivir also preserved the overall structural framework of the polymerase throughout the simulation.

Ligand Flexibility Analysis: To further evaluate the conformational stability of the selected lead compounds and the reference inhibitor during the 100 ns molecular dynamics simulation, the ligand root mean square fluctuation (L-RMSF) was calculated. The RMSF of the ligand gives the information at the residue/atom level of the flexibility of each atom of the ligand when bound in the protein binding pocket and shows how much conformational adaptation is taking place during the simulation (Figure-4).

The complex F3217-0045 showed the lowest ligand flexibility of the compounds studied (Figure-4a). The RMSF values of most of the ligand atoms were found to be in the range of 0.8–1.3Å, while a few terminal atoms showed slightly higher fluctuations in the range of 1.4–1.5Å. The relatively uniform fluctuation profile suggests that the ligand maintained a rigid conformation throughout the simulation indicating strong accommodation in the ATP-binding pocket of JEV RdRp. The limited atomic mobility further corroborates the stable ligand RMSD observed during the trajectory, indicating that only minor local adjustments happened after the initial equilibration.

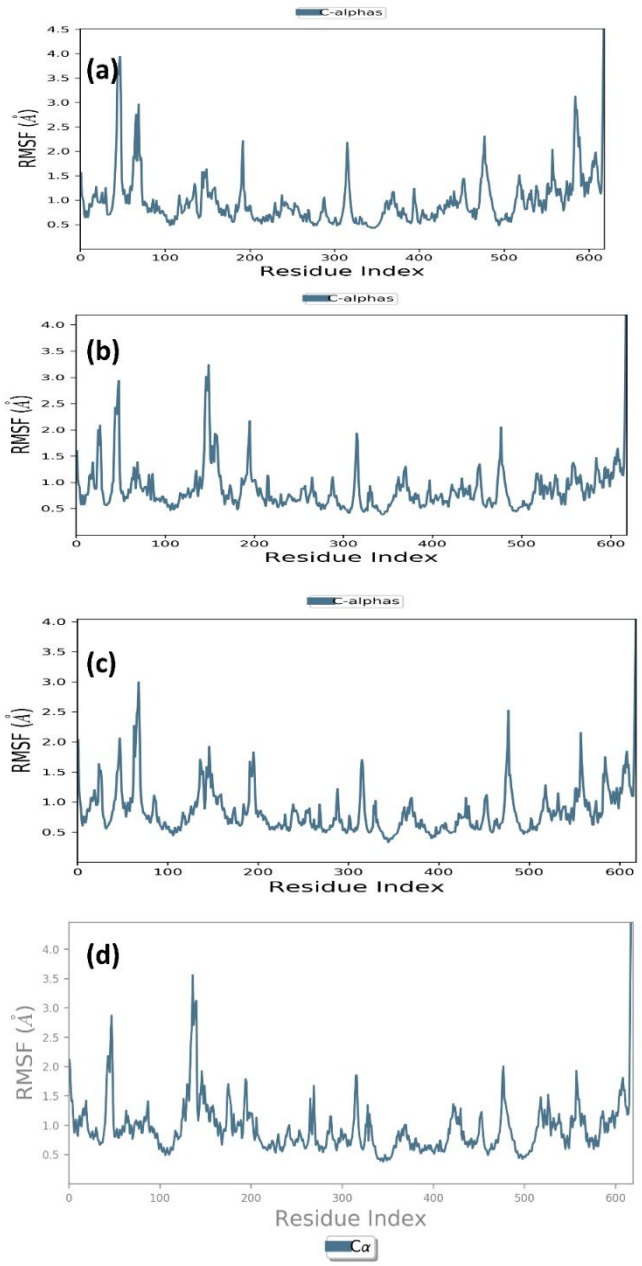

Figure-3: Root mean square fluctuation (RMSF) of JEV RdRp residues during 100 ns molecular dynamics simulation. a) F3217-0045, (b) F1951-0385, (c) F1951-0396, and (d) Galidesivir.

The ligand atoms of F1951-0385 were relatively more flexible than those of F3217-0045 (Figure-4b). The RMSF values were mainly maintained in the range 1.2 to 2.3 Å. Larger fluctuations were observed for the atoms that are located close to one terminal end of the molecule. Some atoms exhibited higher mobility, but the fluctuations were localized and no abrupt increase was seen throughout the ligand structure. This behavior indicates that F1951-0385 maintained the binding orientation but allowed moderate rotation and conformational changes

within the active-site cavity.

The F1951-0396 ligand showed a balanced fluctuation profile, with most of the atoms exhibiting an RMSF below 1.8 Å (Figure-4c). Lower flexibility was found for atoms composing the molecular core while slightly higher fluctuations were found in the periphery substituent region, especially between atoms 17 and 21. However, despite these localized movements, the majority of the ligand remained conformationally stable during the simulation. The limited flexibility observed for F1951-0396 correlates with the stable protein backbone RMSD and low residue fluctuations, suggesting persistent interactions with the catalytic pocket of RdRp.

In contrast, the reference compound Galidesivir showed the highest ligand flexibility in the four systems studied (Figure 4d). The fluctuations of ligand atoms were mostly between 1.9 and 3.0Å and a few atoms had RMSF values close to 3.0Å. A pronounced increase in the mobility was observed in the outer parts of the molecule, suggesting a higher conformational flexibility when attached to the protein. However, the fluctuations were still in the acceptable range for a stable protein-ligand complex and did not suggest ligand dissociation during the simulation.

Radius of Gyration (Rg) and Solvent Accessible Surface Area (SASA) Analysis: Compaction and solvent accessibility of the complexes were analyzed based on the radius of gyration (Rg) and solvent-accessible surface area (SASA) after 100 nanoseconds of molecular dynamics simulations (refer to Figure-5 and 6). The radius of gyration indicates how compact the protein's structure is, while solvent accessibility provides information about solvent exposure and conformational changes during the simulations.

Radius of Gyration (Rg): The radius of gyration of the F3217-0045–RdRp complex remained relatively stable throughout the simulation, fluctuating in a narrow range of ~4.2–4.6 Å (Figure-5a). Small drops were observed at around 25- 30 ns and 40- 45 ns, which were recovered very quickly to the initial values. No increasing or decreasing trend in Rg was observed, indicating that the protein remained in a compact structural organization upon ligand binding and that F3217-0045 did not cause any significant conformational expansion or collapse.

The complex with F1951-0385 showed a slightly larger variation in Rg than the other screened compounds (Figure-5b). The Rg gradually increased during the first half of the simulation and then remained stable at around 3.7-5.0Å from 50 to 70 ns. A small decrease was observed after 75 ns but the value remained stable until the end of the trajectory. In spite of these variations, the overall fluctuations were small indicating that the global protein architecture was maintained during the entire simulation.

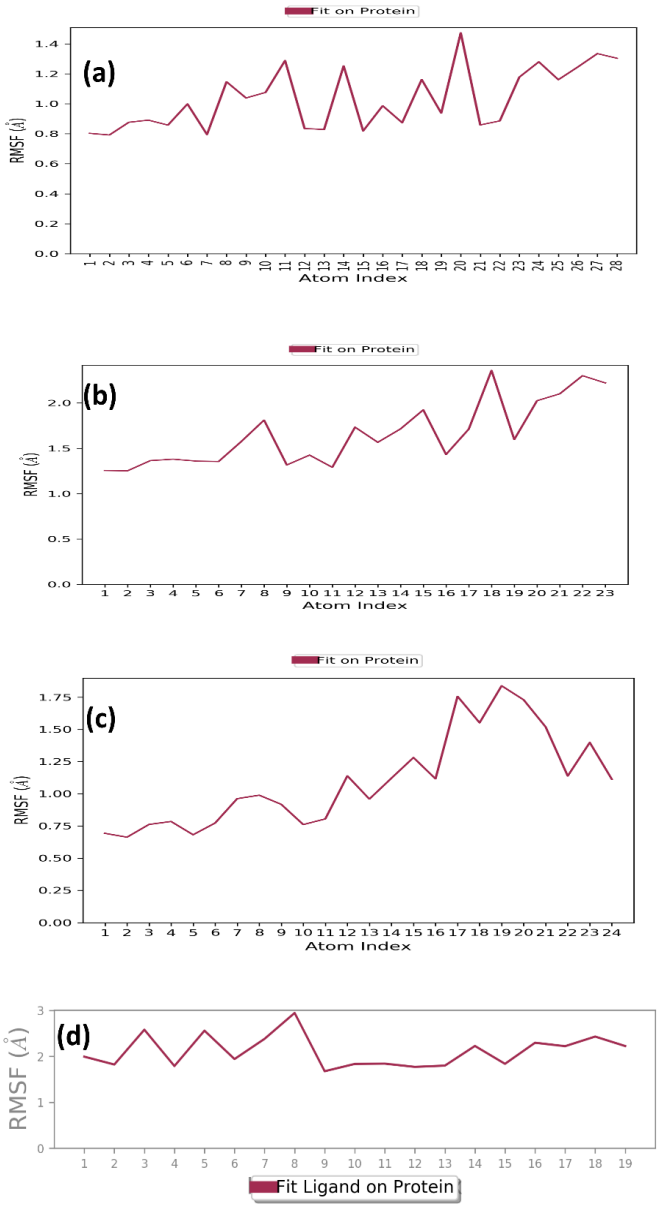

Figure-4: Ligand root mean square fluctuation (Ligand RMSF) of the selected compounds and the reference inhibitor throughout the simulation. (a) F3217-0045, (b) F1951-0385, (c) F1951-0396, and (d) Galidesivir.

The F1951-0396–RdRp complex was found to have the most stable Rg profile among the studied systems (Figure-5c). The radius of gyration was stable at about 3.9–4.0 Å with only small fluctuations during the entire 100 ns simulation. No major expansion or contraction of the structures was observed reflecting good maintenance of protein compactness. The highly stable Rg behavior is consistent with the RMSD and RMSF analyses, further confirming the ability of F1951-0396 to stabilize the RdRp structure during ligand binding.

The Galidesivir–RdRp reference complex also showed stable

radius of gyration during the simulation (Figure-5d). The Rg was close to 3.2-3.3 Å with minor increases after 60 ns and a temporary decrease around 78 ns followed by a rapid return to the equilibrium. These fluctuations were very small and did not suggest any significant changes in protein compactness.

Solvent Accessible Surface Area (SASA): The solvent accessible surface area (SASA) was analyzed to understand the changes in protein surface exposure upon ligand binding (Figure-6). The SASA of the F3217-0045-RdRp complex showed a moderate fluctuation at the beginning of the simulation and then a slow increase after 60 ns with values near 100 $Å^2$ at the end of the simulation (Figure-6a). The progressive increase is due to slight conformational rearrangements increasing the solvent accessibility, but keeping the structural stability of the complex the same.

The SASA fluctuations of the F1951-0385 complex were more pronounced than those of the other screened compounds (Figure-6b). Between 15 and 40 ns, there were clear increases in solvent exposure, followed by transient decreases around 45–55 ns and then stabilization, with values mostly between 70 and 100$Å^2$ for the second half of the simulation. No abrupt structural changes associated with protein unfolding were observed in the complex despite moderate variations of the solvent exposure.

The F1951-0396–RdRp complex showed the most stable SASA profile among the lead compounds investigated (Figure-6c). The SASA values were relatively constant throughout the entire simulation, fluctuating generally between 35 and 65$Å^2$, with only short-lived peaks at around 45 ns and 70 ns. The marginal change in SASA implied that the binding of F1951-0396 preserved the native folding and compactness of the polymerase, while limiting the unnecessary exposure of hydrophobic regions to the solvent.

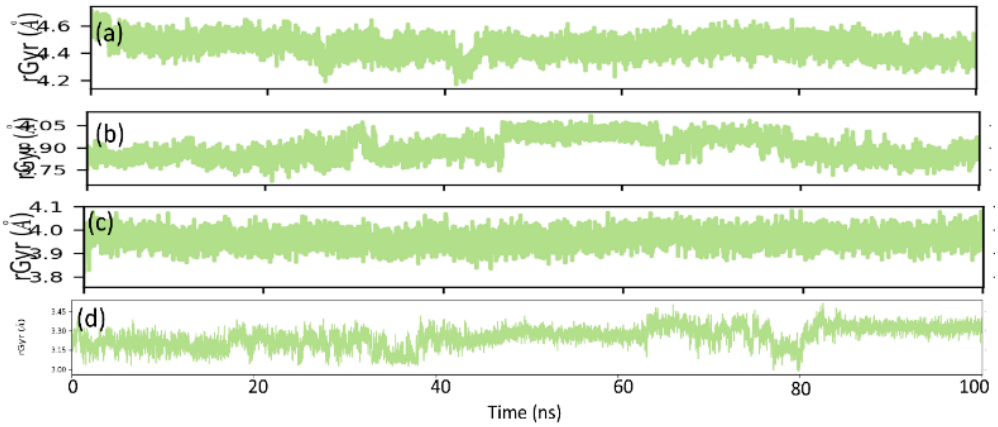

Figure-5: Radius of gyration (Rg) profiles of JEV RdRp complexes during the 100 ns molecular dynamics simulation. (a) F3217-0045, (b) F1951-0385, (c) F1951-0396, and (d) Galidesivir.

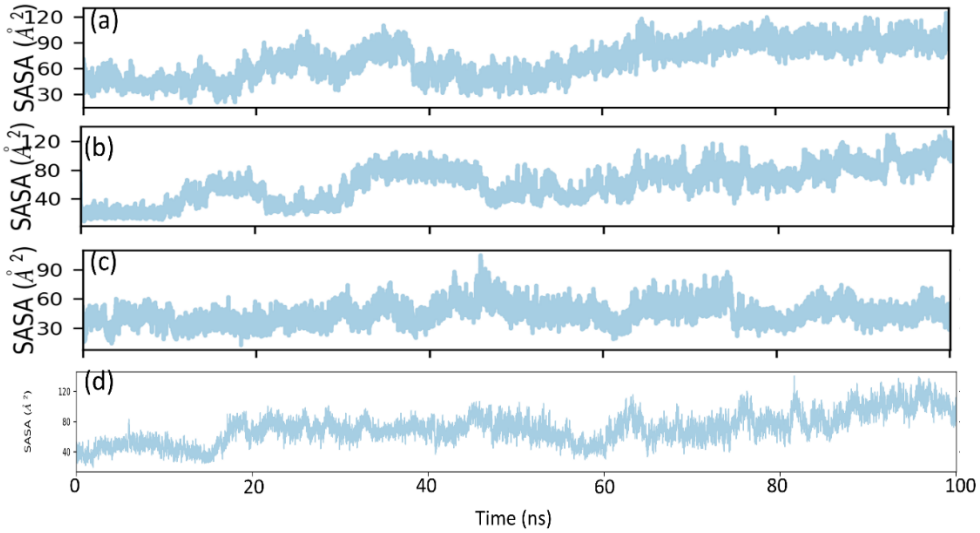

Figure-6: Solvent-accessible surface area (SASA) of JEV RdRp complexes throughout the molecular dynamics simulation.(a) F3217-0045, (b) F1951-0385, (c) F1951-0396, and (d) Galidesivir.

Table-3: Trajectory-based MM/GBSA binding free-energy decomposition of the selected lead compounds and the reference inhibitor, calculated from 100 ns molecular dynamics simulations.

MM/GBSA Energy Decomposition (kcal/mol)	F3217-0045	F1951-0385	F1951-0396	Reference_10445549
ΔG Bind	−84.95 ± 5.71	−60.34 ± 7.80	−53.78 ± 5.74	−34.47 ± 4.07
ΔG Coulomb	−107.50 ± 43.03	−143.96 ± 13.42	−115.08 ± 21.04	−20.54 ± 7.08
ΔG Covalent	2.71 ± 1.66	2.91 ± 1.22	2.33 ± 0.91	3.12 ± 2.09
ΔG Hbond	−6.33 ± 0.99	−7.28 ± 0.81	−5.45 ± 0.72	−2.25 ± 0.91
ΔG Lipophilic	−24.36 ± 1.18	−12.54 ± 2.67	−14.47 ± 1.16	−7.30 ± 1.12
ΔG SolvGB	108.07 ± 38.82	138.77 ± 14.54	121.67 ± 17.48	26.49 ± 3.85
ΔG van der Waals	−52.04 ± 2.49	−37.84 ± 2.81	−42.10 ± 2.67	−32.89 ± 2.75
Ligand Strain Energy	3.19 ± 1.81	4.03 ± 1.80	3.12 ± 0.98	3.82 ± 1.92

Higher fluctuations in SASA were observed for the Galidesivir bound complex (Figure-6d). Around 15 ns, there was an increase in solvent accessibility, followed by dynamic oscillations during the remainder of the simulation. During the last phase of the trajectory, SASA values increased gradually up to ~100–120Å² signifying a greater conformational flexibility of the protein surface than the screened lead compounds. However, these fluctuations were within the allowable range for a stable protein-ligand complex.

Generally, all the four JEV RdRp complexes were stable in 100 ns molecular dynamics simulation without any major structural perturbations after ligand binding. Analyses of RMSD, RMSF, ligand RMSF, Rg and SASA consistently demonstrated the catalytic core was largely intact and fluctuations were mostly limited to flexible loop and terminal regions. F1951-0396 exhibited the greatest dynamic stability amongst the compounds studied with stable protein and ligand conformations, low residue fluctuations and consistent compactness followed by F3217-0045. While F1951-0385 and the reference Galidesivir exhibited relatively higher ligand mobility and solvent exposure, both maintained stable interactions within the binding pocket during the simulation. These findings suggest that F1951-0396 and F3217-0045 are the most promising lead compounds for targeting JEV RdRp.

Trajectory-Based MM/GBSA Binding Free Energy Analysis: To further evaluate the binding stability of the selected lead compounds during the molecular dynamics simulation, trajectory-based MM/GBSA calculations were also performed on the extracted snapshots from the 100 ns trajectories. The total binding free energy (ΔG_bind) and the individual energy terms are listed in Table-3.

F3217-0045 was the compound with the best binding free energy (ΔG_bind of −84.95 ± 5.71 kcal/mol) among the studied compounds showing the strongest binding affinity toward JEV RdRp. This favorable binding was mainly governed by significant Coulombic (−107.50 ± 43.03 kcal/mol), van der Waals (−52.04 ± 2.49 kcal/mol), and lipophilic (−24.36 ± 1.18 kcal/mol) interactions besides favorable hydrogen-bond contributions (−6.33 ± 0.99 kcal/mol). The polar solvation energy was unfavorable for binding (108.07 ± 38.82 kcal/mol), but the favorable intermolecular interactions were greater than the unfavorable contribution and gave the lowest binding free energy of all the complexes.

The F1951-0385 complex was found to have the second best binding affinity with ΔG_bind = −60.34 ± 7.80 kcal/mol. This complex was characterized by the strongest electrostatic interaction (ΔG_Coulomb = −143.96 ± 13.42 kcal/mol) and the largest hydrogen-bond contribution (−7.28 ± 0.81 kcal/mol) among all screened compounds. However, the favorable interactions mentioned above were somewhat countered by a relatively high polar solvation energy (138.77 ± 14.54 kcal/mol), which led to a less favorable overall binding free energy than F3217-0045.

F1951-0396 had a ΔG_bind of −53.78 ± 5.74 kcal/mol, which is still significantly more favorable than the reference compound. The binding of this ligand was mainly stabilized by a Coulombic (−115.08 ± 21.04 kcal/mol), van der Waals (−42.10 ± 2.67 kcal/mol) and lipophilic (−14.47 ± 1.16 kcal/mol) interaction with a positive contribution of hydrogen-bond energy (−5.45 ± 0.72 kcal/mol). The overall binding affinity was lower than those of F3217-0045 and F1951-0385, but its stable interaction with the catalytic pocket throughout the simulation is supported by consistent energetic contributions.

The reference compound (Galidesivir) showed the highest unfavorable binding free energy (−34.47±4.07kcal/mol). The van der Waals contribution (−32.89±2.75kcal/mol) was relatively favorable, but the electrostatic (−20.54±7.08 kcal/mol), lipophilic (−7.30±1.12 kcal/mol) and hydrogen-bond (−2.25±0.91kcal/mol) contributions were weaker, resulting in a much lower binding affinity than the screened lead compounds.

Finally, the MM/GBSA analysis from the trajectory revealed that all the three selected compounds possess considerably higher binding affinities towards JEV RdRp compared to the reference inhibitor. The most favorable binding free energy was found for Compound F3217-0045, followed by F1951-0385 and F1951-0396, suggesting that these compounds are prone to form energetically stable interactions in the polymerase active site. These results, together with the molecular dynamics analyses, also provide further evidence for the potential of F3217-0045 and F1951-0396 as promising lead candidates for the development of novel inhibitors targeting the JEV RNA-dependent RNA polymerase.

Results and Discussion

The present study identified F3217-0045, F1951-0385, and F1951-0396 as potential inhibitors of JEV RdRp, with all three compounds showing stronger trajectory-based MM/GBSA binding energies than the reference compound Galidesivir. Among these, F3217-0045 showed the most favorable ΔG_bind value of −84.95 ± 5.71 kcal/mol, followed by F1951-0385 (−60.34 ± 7.80 kcal/mol) and F1951-0396 (−53.78 ± 5.74 kcal/mol), while Galidesivir exhibited a weaker binding energy of −34.47 ± 4.07 kcal/mol. The stronger binding of the selected hits was mainly driven by favorable Coulombic, van der Waals, lipophilic and hydrogen-bond energy terms.

These findings are in agreement with previous studies that have identified JEV RdRp as a promising antiviral target. In a structural study, researchers demonstrated that JEV RdRp recognizes ATP/GTP in the nucleotide-binding region, and suggested that disruption of nucleotide binding may interfere with initiation of RNA synthesis, supporting the rationale for targeting the ATP/GTP-binding pocket used in the present work [8].

Our results are in agreement with the results of a recent study which screened neem derived bioflavonoids against JEV RdRp and observed stable binding of Gedunin, Nimbolide, Ohchinin acetate and Kulactone with the RdRp through interactions with key residues such as Arg474, Asp668 and Trp800 during 100 ns MD simulation[27]. The selected compounds in the present study also interacted with key pocket residues such as Arg460, Lys463, Arg474, Arg742, Trp477, Trp800, Ser801, and Ile802, suggesting that the identified ligands occupy a functionally relevant region of RdRp.

Our lead compound F3217-0045 had a comparable binding energy profile (−84.95 ± 5.71 kcal/mol) compared to Echinacea angustifolia which was studied with Echinacoside, Echinacin and Rutin, which showed robust binding energies with MM/GBSA in the vicinity of −80 kcal/mol with positive Coulombic, lipophilic and van der Waals contributions [28]. Likewise, four marine-derived compounds in the 2024 marine brown algae study exhibited promising docking energies and robust 200 ns MD behavior relative to Galidesivir, consistent with the general finding that natural-product-like and antiviral-enriched chemical scaffolds can stably bind to the JEV RdRp pocket[29].

Our findings are also consistent with recent computational studies on JEV RdRp. The researchers reported three repurposed anti-dengue compounds with promising binding free energies and stable 100 ns molecular dynamics trajectories emphasizing the potential of drug repurposing for JEV therapy [30]. Alam and his co-workers also identified phytochemicals from the Zingiberaceae family that exhibited good docking affinities and stable interactions with the RdRp active site[31]. Similar to these studies, the lead compounds identified in this work demonstrated stable binding during the simulation and good binding free energies compared to the reference inhibitor Galidesivir. However, unlike previous studies focusing on repurposed drugs or phytochemicals, our study searched an antiviral-focused chemical library, which resulted in the identification of structurally distinct lead compounds with promising potential for further experimental validation against JEV RdRp.

Crucially, while most of the previous work was based on natural compounds from neem, echinacea, Zingiberaceae or marine algae, the present work explored an antiviral focused screening library enriched with molecules related to known bioactive antiviral compounds. This strategy increases the chemical diversity of potential JEV RdRp inhibitors beyond plant or marine-derived scaffolds. However, F1951-0396 exhibited the most consistent dynamic stability according to RMSD, RMSF, Rg, and SASA profiles, though F3217-0045 had the highest MM/GBSA binding energy. In addition, F3217-0045 and F1951-0396 are the best candidates, energetically favored and dynamically favored, respectively. These compounds should be considered for experimental enzymatic and cell-based validation against JEV replication.

Conclusion

In this study, we performed a comprehensive structure based virtual screening to identify novel inhibitors against JEV-RdRp. Based on the binding affinities and interaction profiles of the screened compounds, the three most promising compounds were F3217-0045, F1951-0385 and F1951-0396. Stability of all the three protein-ligand complexes during 100 ns simulation time was also confirmed by molecular dynamics simulations. Trajectory analyses such as RMSD, RMSF, ligand RMSF, radius of gyration, SASA and MM/GBSA calculations consistently showed that the identified compounds were stable in interactions inside the ATP-binding pocket of JEV RdRp. Interestingly, the binding free energy of F3217-0045 was the best, while the conformation stability of F1951-0396 was the best in the molecular dynamics simulations, indicating that these compounds are promising starting points for the development of drugs against JEV.

Although these results are promising, the present study is solely

based on computational approaches and the predicted inhibitory activity needs to be validated experimentally. Future studies should include biochemical assays for polymerase inhibition, anti-viral evaluation in JEV-infected cell culture models, cytotoxicity and selectivity studies and pharmacokinetic and ADMET profiling to determine the drug-like properties of the identified compounds. Additionally, structure–activity relationship (SAR) studies and medicinal chemistry optimization can be conducted to improve potency, selectivity and drug-like properties. Given the conserved architecture of flaviviral RdRp enzymes, these lead compounds may also serve as a basis for the development of broad-spectrum antivirals against other clinically important flaviviruses including dengue, West Nile, yellow fever and Zika viruses. In summary, the results of this study offer a strong computational foundation for the future discovery and improvement of RdRp-targeted therapies against Japanese encephalitis and related flaviviral infections.

References

1. Solomon T. (2006). Control of Japanese Encephalitis-Within Our Grasp?. *New England Journal of Medicine*, 355(9), 869–871 (2006).

2. Campbell G., Hills S., Fischer M., Jacobson J., Hoke C., Hombach J., Marfin A., Solomon T., Tsai T., Tsui, V. and Ginsburg A. (2011). Estimated global incidence of Japanese encephalitis: a systematic review. *Bulletin of the World Health Organization*, 89, 766-774.

3. Harshani H.B.C. and Abeynayake J.I. (2025). Japanese encephalitis in Asia: A comprehensive review. *Journal of Vector Borne Diseases*, 62(4), 398–407.

4. Turtle L. and Solomon T. (2018). Japanese encephalitis — the prospects for new treatments. *Nature Reviews Neurology*, 14(5), 298–313(2018).

5. Best S.M. (2016). Flaviviruses. *Current Biology*, 26(24), R1258–R1260.

6. Lindenbach B.D. and Rice C.M. (2003). Molecular biology of flaviviruses. *Advances in virus research*, 59, 23–62.

7. Pierson T.C. and Diamond M.S. (2020). The continued threat of emerging flaviviruses. *Nature Microbiology*, 5(6), 796–812.

8. Surana P., Satchidanandam V. and Nair D.T. (2014). RNA-dependent RNA polymerase of Japanese encephalitis virus binds the initiator nucleotide GTP to form a mechanistically important pre-initiation state. *Nucleic acids research*, 42(4), 2758–2773(2014).

9. Malet H., Massé N., Selisko B., Romette J. L., Alvarez K., Guillemot J.C., Tolou H., Yap T.L., Vasudevan S.G. and Lescar J. (2008). The flavivirus polymerase as a target for drug discovery. *Antiviral research*, 80(1), 23–35.

10. Furuta, Y., Komeno, T., & Nakamura, T. (2017). Favipiravir (T-705) (2017). A broad spectrum inhibitor of viral RNA polymerase. *Proceedings of the Japan Academy, Series B*, 93(7), 449-463.

11. Furuta Y., Gowen B.B., Takahashi K., Shiraki K., Smee D.F. and Barnard D.L., Favipiravir (T-705) (2013). A novel viral RNA polymerase inhibitor. *Antiviral Research*, 100(2), 446–454(2013).

12. Eyer L., Nencka R., De Clercq E., Seley-Radtke K. and Růžek D. (2018). Nucleoside analogs as a rich source of antiviral agents active against arthropod-borne flaviviruses. *Antiviral Chemistry and Chemotherapy*, 26, 2040206618761299.

13. Burley S.K., Bhatt R., Bhikadiya C., Bi C., Biester A., Biswas P., Bittrich S., Blaumann S., Brown R. and Chao H. (2025). Updated resources for exploring experimentally-determined PDB structures and Computed Structure Models at the RCSB Protein Data Bank. *Nucleic Acids Research*, 53(D1), D564–D574, (2025).

14. Madhavi Sastry G., Adzhigirey M., Day T., Annabhimoju R. and Sherman W. (2013). Protein and ligand preparation: parameters, protocols, and influence on virtual screening enrichments. *Journal of Computer-Aided Molecular Design*, 27(3), 221–234.

15. Roos K., Wu C., Damm W., Reboul M., Stevenson J. M., Lu C., Dahlgren M.K., Mondal S., Chen W. and Wang L. (2019). OPLS3e: Extending force field coverage for drug-like small molecules. *Journal of chemical theory and Computation*, 15(3), 1863–1874, (2019).

16. Schrödinger (2025). Schrödinger Release 2025-1: LigPrep LLC, New York, NY.

17. Halgren T. A., Murphy R.B., Friesner R.A., Beard H.S., Fry L.L., Pollard W.T. and Banks, J. L. (2004). Glide: a new approach for rapid, accurate docking and scoring. 2. Enrichment factors in database screening. *Journal of medicinal chemistry*, 47(7), 1750–1759, (2004).

18. Friesner R.A., Murphy R.B., Repasky M.P., Frye L.L., Greenwood J.R., Halgren T.A., Sanschagrin P.C. and Mainz D.T. (2006). Extra precision glide: Docking and scoring incorporating a model of hydrophobic enclosure for protein− ligand complexes. *Journal of medicinal chemistry*, 49(21), 6177–6196.

19. Halgren T.A., Murphy R.B., Friesner R.A., Beard H.S., Frye L.L., Pollard W.T. and Banks J. L. (2004). Glide: A New Approach for Rapid, Accurate Docking and Scoring. 2. Enrichment Factors in Database Screening. Journal of Medicinal Chemistry, 47(7), 1750–1759.

20. Friesner R. A., MurphyR. B., Repasky M. P., Frye L. L., Greenwood J. R., Halgren T. A., Sanschagrin P. C. & and Mainz D. T. (2006). Extra precision glide: Docking and scoring incorporating a model of hydrophobic enclosure for protein−ligand complexes. *Journal of Medicinal Chemistry*,

49(21), 6177–6196.

21. Schrödinger (2025). Schrödinger Release 2025-1: Prime. LLC, New York, NY.

22. Bowers K. J., Chow D. E., Xu H., Dror R. O., Eastwood M. P., Gregersen B. A., Klepeis J. L., Kolossvary I., Moraes M. A., Sacerdoti F. D., Salmon J. K., Shan Y. and Shaw D. E. (2006). Scalable Algorithms for Molecular Dynamics Simulations on Commodity Clusters. IEEE, Tampa, FL.

23. Evans D. J. and Holian B. L. (1985). The nose–hoover thermostat. The Journal of chemical physics, 83(8), 4069–4074.

24. Janek J. and Kolafa J. (2024). Novel barostat implementation for molecular dynamics. *The Journal of Chemical Physics*, 160(18).

25. Kräutlerr V., Van Gunsteren W. F. and Hünenberger P. H. (2001). A fast SHAKE algorithm to solve distance constraint equations for small molecules in molecular dynamics simulations. Journal of Computational Chemistry, 22(5), 501–508.

26. Julander J. G., Demarest J. F., Taylor R., Gowen B. B., Walling D. M., Mathis A. and Babu Y. S. (2021). An update on the progress of galidesivir (BCX4430), a broad-spectrum antiviral. *Antiviral Research*, 195, 105180.

27. Dwivedi V. D., Singh A., El-Kafraway S. A., Alandijany T. A., Faizo A. A., Bajrai L. H., Kamal M. A. and Azhar E. I. (2021). Mechanistic insights into the Japanese encephalitis virus RNA dependent RNA polymerase protein inhibition by bioflavonoids from Azadirachta indica. *Scientific Reports*, 11(1), 18125.

28. Yadav P., El-Kafrawy S. A., El-Day M. M., Alghafari W. T., Faizo A. A., Jha S. K., Dwivedi V. D. and Azhar, E. I. (2022). Discovery of Small Molecules from Echinacea angustifolia Targeting RNA-Dependent RNA Polymerase of Japanese Encephalitis Virus. *Life*, 12(7), 952.

29. Alshammari S. O. (2024). Marine Brown Algae-Derived Compounds as Potential Inhibitors of Japanese Encephalitis Virus RNA-Dependent RNA Polymerase. Marine Drugs, 22(2), 92.

30. Bajrai L. H., Alandijany T. A., Alsaady I., El-Daly M. M., Tolah A. M., Khateb A. M., Dubey A., Dwivedi V. D. and Azhar E. I. (2024). Assessing the inhibitory potential of anti-dengue compounds against Japanese encephalitis virus RNA dependent RNA polymerase: An in silico study. *Journal of Biomolecular Structure and Dynamics*, 42(21), 11844–11860.

31. Alam A., Anjum A., Moglad E. H., Jawaid T., Foudah A. I., Alotaibi F., Aba Alkhayl F. F., Azhar Kamal M., Warsi M. K. and Balaha M. F. (2025). Zingiberaceae-derived phytomolecules inhibit Japanese encephalitis virus RNA dependent RNA polymerase: a molecular dynamics study. *Journal of Biomolecular Structure and Dynamics*, 43(16), 8944–8958.